On the Slices-based Limit Equilibrium Method for the Active Earth Pressure Applied by Soils with Nonlinear Strength Behavior

Zhongzhi Fu[1], Shengshui Chen[2], Guoying Li[3]
1-Senior Engineer, Geotechnical Engineering Department, Nanjing Hydraulic Research Institute, Nanjing 210024, China
2- Professor, Key Laboratory of Failure Mechanism and Safety Control Techniques of Earth- Rock Dams, Ministry of Water Resource, Nanjing 210029, China
3-Professor, Geotechnical Engineering Department, Nanjing Hydraulic Research Institute, Nanjing 210024, China

Email: fu_zhongzhi@yahoo.com

Abstract

The slices-based limit equilibrium method was used to study the active earth pressure applied by soils with nonlinear strength behavior. An iterative scheme and a local minimization process were employed to consider the dependence of the peak friction angle on the normal effective stress and the mathematical nature of the active earth pressure, respectively. The preference of iterative variable for local minimization processes as well as the influence of the distribution of interslice force angles on the active earth pressure and its points of application were discussed. Numerical examples show that the slices-based limit equilibrium method is reliable in predicting static and dynamic active earth pressures upon vertical or sloping retaining walls for soils with both linear and nonlinear failure criteria. The use of nonlinear strength parameters in the slices-based method was also discussed.
Keywords: Active Earth Pressure, Retaining Wall, Limit Equilibrium, Generalized Slice Method.

1. INTRODUCTION

The active earth pressure problem is an important and classical issue in soil mechanics that deals with the stability of a retaining structure and the backfilled soils. The two major early theories to estimate the active (and passive) earth pressure values are those by Coulomb (1776) and by Rankine (1857) as summarized in standard textbooks (e.g. Smith and Smith 1998). Both theories are recommended in designing specifications for retaining structures and are very much in use in geotechnical engineering. Other theories for earth pressure problems include the slices-based limit equilibrium method (Rahardjo and Fredlund 1984; Chen and Li 1998), the limit analysis method (Chen 1975; Yang 2007) and the slip line method (Liu and Wang 2008; Peng and Chen 2013) as summarized by Sun and Song (2016). In most of these works, the peak shear stress that a surface can sustain is assumed linearly dependent upon the normal effective stress applied, which makes them inapplicable to earth pressure problems where the retained soils exhibit strong nonlinear strength behavior.

The above situation is often encountered in rockfill dams. Fig.1 (a) depicts a retaining wall truncating the downstream slope of a rockfill dam built on a sloping mountain for a pumped storage station, so as to considerably reduce the amount of rockfill materials needed (Liu et al. 2008). A retaining wall is also used sometimes to truncate the upstream slope so as to avoid building the toe plinth on an unsatisfactory foundation such as a fault as shown in Fig. 1(b) (Fu et al. 2014). Designing such retaining structures needs the information about the active earth pressure exerted by the backfilled rockfill materials. It is well known that the strength of coarse granular materials, like gravels and rockfills, depends on the normal stress or the confining pressure (Leps 1970; Maksimovic 1989; Xiao et al. 2014). For instance, the peak friction angle (φ) of a stressed rockfill in triaxial compression can be well approximated by the following equation (Liu et al. 2008):

$$\varphi = \varphi_0 - \Delta\varphi \lg\left(\frac{\sigma_3}{p_a}\right) \qquad (1)$$

In which $\varphi = \sin^{-1}[(\sigma1-\sigma3)/(\sigma1+\sigma3)]$, and $\sigma1$ and $\sigma3$ are the maximum principal stress and the minimum one, respectively. $\varphi0$ and $\Delta\varphi$ are two parameters, and p_a denotes the atmospheric pressure (p_a = 101325 Pa). Because the peak friction angle of the retained soils along a given failure surface is not known a priori, the widely used Rankine theory and Coulomb theory as well as other analytical approaches cannot be directly used in most circumstances.

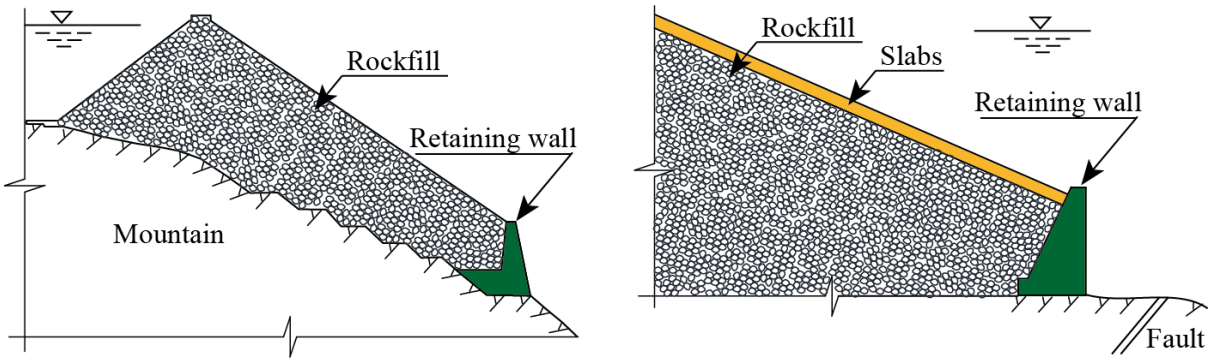

(a) Used downstream (b) Used upstream

Fig. 1. Useof retaining walls in concrete face rockfill dams

Multilayered soil strata and complex topography as well as variable loading conditions sometimes result in extra difficulty in using classical earth pressure theories, and therefore numerical methods exemplified by the finite element method and the finite difference method have been increasingly used in solving earth pressure problems (Potts and Fourie 1986; Bhatia and Bakeer 1989; Benmeddour et al. 2012; Worden and Achmus 2013). Certain constitutive models were required to represent the stress ~ strain behavior of the retained soils and therefore much more parameters were inevitably needed, obtaining more information but meanwhile adding expense and uncertainty to such numerical analyses. Early endeavor was also exercised in predicting the active earth pressure using the slices-based limit equilibrium analysis (Rahardjo and Fredlund 1984; Chen and Li 1998; Zakerzadeh et al. 1999). However, the nonlinear strength behavior of the retained soils was seldom considered in earth pressure problems, despite of their wide consideration in slope stability analysis (Collins et al. 1988; Zhang and Chen 1987; Jiang et al. 2003).

Recently, the nonlinear strength behavior of soils was considered in using the upper bound limit analysis method (Yang 2007) and the slip line method (Sun and Song 2016) for active earth pressure problems. A common advantage of both methods is the unnecessity of introducing any assumption for the interslice forces as in those slices-based limit equilibrium methods (Rahardjo and Fredlund 1984; Chen and Li 1998; Zakerzadeh et al. 1999). However, in the method by Yang (2007), the nonlinear strength of soils is only reflected in an average manner since a single and constant apparent friction angle (φ_t) is used along the failure surface in evaluating the internal energy dissipation. The method by Sun and Song (2016) can consider the variation of the shear strength along the failure surface. However, it cannot reflect the influence of the flexibility of retaining structures upon the active earth pressure, since for each failure surface a single and unique active earth pressure can be obtained.

Since the slices-based limit equilibrium analysis is among the most widely used methods in geotechnical engineering, and its ability in seeking the active earth pressure applied by soils with linear strength behavior has already been demonstrated by several authors (Rahardjo and Fredlund 1984; Chen and Li 1998; Zakerzadeh et al. 1999), it is natural to extend this popular method for soils with nonlinear shear strength. In this paper, the generalized method of slices (Chen and Morgenstern 1983; Chen and Li 1998) was extended for this particular aim. The equilibrium equations derived by Chen and Morgenstern (1983) were used. An iterative cycle was incorporated so as to obtain the mobilized strength of soils that is compatible with the normal stress along the failure surface. In addition, a local minimization process was performed to seek the minimum active earth pressure for each possible failure surface. Some cases were studied and the results were compared with those obtained by other methods. The selection of the iterative variable for the local minimization processes was discussed, and the influence of the interslice force angle as well as the type of failure surfaces on the solutions were studied. Nonlinear strength parameters used for the slices-based limit equilibrium analysis were also discussed.

2. LIMIT EQUILIBRIUM EQUATIONS AND THE SOLUTION STRATEGY

For the sake of integrity and familiarity of notations, the equilibrium equations of the retained soil mass were simply presented in this part. The slope-retaining wall system was shown in Fig. 2, in which the retaining surface of the wall was assumed vertical tentatively. The active earth pressure applied upon a sloping surface can also be calculated using the vertical slices-based method as will be shown later. Before introducing the force and moment equilibrium equations, the forces that a typical soil slice (width = dx) bears were summarized as follows:

1. vertical body force, dW, and horizontal body force, dQ;
2. surcharge perpendicular to the free surface, $q(x)$;
3. normal force, dN, and shear force, dT, upon the bottom failure surface;
4. interslice forces, G and G+dG, exerted by the neighboring slices.

Other symbols in Fig. 2 include the height of the retaining wall, H; the inclination of the failure surface measured from the horizontal plane, α; the inclination of the action line of G denoted by β; the inclination of the free surface, δ, the vertical coordinate of the application point of G denoted by y_t, and the vertical distance between the action line of dQ and the bottom of the slice denoted by h_e. The elevation of the failure surface and that of the free surface were represented by the function $y = y(x)$ and $z = z(x)$, respectively.

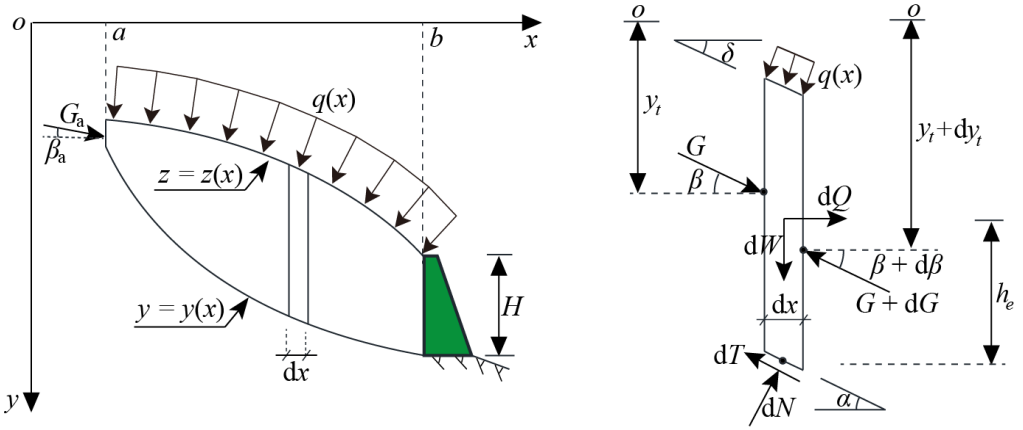

(a) The slope-retaining wall system (b) Forces upon a soil slice

Fig. 2. The slope-retaining wall system and forces upon a soil slice

2.1. FORCE AND MOMENT EQUILIBRIUM EQUATIONS

The horizontal andvertical force equilibrium conditionsof the soil slice read:

$$\left.\begin{aligned} &\mathrm{d}N\sin\alpha-\mathrm{d}T\cos\alpha+G\cos\beta-(G+\mathrm{d}G)\cos(\beta+\mathrm{d}\beta)+\mathrm{d}Q-q\tan\delta\mathrm{d}x=0\\ &-\mathrm{d}N\cos\alpha-\mathrm{d}T\sin\alpha+G\sin\beta-(G+\mathrm{d}G)\sin(\beta+\mathrm{d}\beta)+\mathrm{d}W+q\mathrm{d}x=0\end{aligned}\right\} \quad (2)$$

For the sake of universality, the following failure criterion was used to describe the stress state of soils along the failure surface $y = y(x)$:

$$\mathrm{d}T=(\mathrm{d}N-u\cdot\mathrm{d}x\sec\alpha)\tan\varphi+c\cdot\mathrm{d}x\sec\alpha \quad (3)$$

In which c and φ are the cohesion and the friction angle of the soil, respectively. u is the porepressure along the failure surface. For most coarse granular materials, $c = 0$ and φ is a nonlinear function of the normal effective stress. Solving dN and dT from Eq. (2) and substituting them into Eq. (3) yield the following differential equation for the interslice force, G (Chen 2003):

$$\cos(\varphi-\alpha+\beta)\frac{\mathrm{d}G}{\mathrm{d}x}-G\sin(\varphi-\alpha+\beta)\frac{\mathrm{d}\beta}{\mathrm{d}x}=-p(x) \quad (4)$$

in which

$$p(x)=\left(\frac{\mathrm{d}W}{\mathrm{d}x}+q\right)\sin(\varphi-\alpha)-\left(\frac{\mathrm{d}Q}{\mathrm{d}x}-q\tan\delta\right)\cos(\varphi-\alpha)-u\cdot\sin\varphi\sec\alpha+c\cdot\cos\varphi\sec\alpha \qquad (5)$$

The moment equilibrium equation of the soil slice that around the center of the failure surface can also be derived (Chen 2003), that is

$$G\sin\beta=\frac{\mathrm{d}}{\mathrm{d}x}(y_t\cdot G\cos\beta)-y\frac{\mathrm{d}}{\mathrm{d}x}(G\cos\beta)+\frac{\mathrm{d}Q}{\mathrm{d}x}h_e-q\tan\delta(y-z) \qquad (6)$$

Eqs. (4) and (6) govern the equilibrium of the differential soil slice, which, combined with certain boundary conditions, can be solved analytically or numerically. For the active earth pressure problem depicted in Fig. 1, the following boundary conditions can be introduced:

$$\left.\begin{aligned} &y(x=a)=Y_a;\quad \beta(x=a)=\beta_a;\quad G(x=a)=G_a;\quad y_t(x=a)=T_a\\ &y(x=b)=Y_b;\quad \beta(x=b)=\beta_b \end{aligned}\right\} \qquad (7)$$

The unknown variables to be sought are the force acted at the right boundary ($x=b$) and its point of application denoted by the following notations:

$$G(x=b)=G_b;\quad y_t(x=b)=T_b \qquad (8)$$

The force applied at the left boundary, G_a, is considered herein for generality. In addition, β_b depends on the roughness of the wall and is generally set to the friction angle between the soil and the retaining wall under an active condition.

2.2. THE SOLUTION STRATEGY

Eq. (4) is a linear nonhomogeneous first-order ordinary differential equation (Kreyszig 2010), the solution of which can be derived following a standard procedure (Chen 2003):

$$G(x)=\exp\left[\int_a^x\tan(\varphi-\alpha+\beta)\mathrm{d}\beta\right]\cdot\left[G_a-\int_a^x p(\xi)s(\xi)\mathrm{d}\xi\right] \qquad (9)$$

in which

$$s(x)=\sec(\varphi-\alpha+\beta)\exp\left[-\int_a^x\tan(\varphi-\alpha+\beta)\mathrm{d}\beta\right] \qquad (10)$$

Therefore, it is easy to obtain the explicit expression for the earth pressure at the right boundary, Gb:

$$G_b=\exp\left[\int_a^b\tan(\varphi-\alpha+\beta)\mathrm{d}\beta\right]\cdot\left[G_a-\int_a^b p(x)s(x)\mathrm{d}x\right] \qquad (11)$$

As can be seen from Eq. (11) and expressions of the functions $p(x)$ and $s(x)$, the active earth pressure depends on the location of the failure surface (via the functions $\alpha(x)$ and $y(x)$) and the interslice force angle function $\beta(x)$. Mathematically, this is a problem of seeking an extreme of the functional, and the standard approach is to apply the so-called Euler-Lagrange condition (Andrews and Phillips 2004). However, such an analytical approach generally leads to some highly nonlinear ordinary differential equations of $\alpha(x)$ and $\beta(x)$, which are almost unsolvable. In addition, it will be shown later that for practical problems the extreme of Eq. (11) can be achieved often at places other than the stationary points due to the constraints of some boundary conditions. Therefore, the extreme of Eq. (11) was obtained numerically in this study.

Eq. (6) can also be integrated as follows (Chen 2003):

$$\begin{aligned}&(y_t-y)\cdot G\cos\beta-(T_a-Y_a)\cdot G_a\cos\beta_a\\&=\int_a^x\left[G(\sin\beta-\tan\alpha\cos\beta)-\frac{\mathrm{d}Q}{\mathrm{d}x}h_e+q\tan\delta(y-z)\right]\mathrm{d}\xi\end{aligned} \qquad (12)$$

which, by introducingthe boundary conditions given in Eqs. (7) and (8), can be rewritten as follows:

$$G_b t_b \exp\left[-\int_a^b \tan(\varphi_e - \alpha + \beta)\,\mathrm{d}\beta\right] + \int_a^b p(x)s(x)t(x)\,\mathrm{d}x - M_e = 0 \tag{13}$$

in which

$$t(x) = \int_a^x (\sin\beta - \tan\alpha\cos\beta)\exp\left[\int_a^\xi \tan(\varphi_e - \alpha + \beta)\,\mathrm{d}\beta\right]\mathrm{d}\xi \tag{14}$$

and

$$M_e = (T_b - Y_b)\cdot G_b\cos\beta_b - (T_a - Y_a)\cdot G_a\cos\beta_a + \int_a^b \left[\frac{\mathrm{d}Q}{\mathrm{d}x}h_e - q\tan\delta(y-z)\right]\mathrm{d}x \tag{15}$$

The concept of seeking an extreme of the active earth pressure is similar to that in safety factor evaluation in slope stability problems. Assume that the location of the failure surface is known so that the functions $y(x)$ and $\alpha(x)$ are determined, varying the function $\beta(x)$ within the valid range will yield a local minimum of Gb, which can be further substituted into Eq. (13) to get its point of application (Tb). Traversing all the possible locations of the failure surfaces and repeatedly implementing the optimization processes, we can obtain a series of local minimums of Gb. The physically meaningful active earth pressure will be the maximal one of those local minimums. Therefore, the cornerstone here is to select the function $\beta(x)$ that minimizes the earth pressure for a given failure surface.

The influence of the interslice force angle function $\beta(x)$ was studied by a few authors (Chen 2003; Zakerzadeh et al. 1999). Zakerzadeh et al. (1999) suggested that a reasonable active earth pressure could be obtained when using an interslice force function that varies linearly from the starting point of the failure surface (a in Fig. 2) to the end point of the failure surface (b in Fig. 2). Chen and Morgenstern (1983) and Chen (2003) suggested a more general form as follows:

$$\tan\beta = f_0(x) + \lambda\cdot f(x) \tag{16}$$

herein λ is a scalar, and $f0(x)$ and $f(x)$ are two independent functions. A reasonable choice of the functions that satisfies the boundary conditions strictly was given by Chen (2003), that is

$$f_0(x) = \frac{\tan\beta_b - \tan\beta_a}{b-a}(x-a);\quad f(x) = \sin\frac{\pi}{b-a}(x-a) \tag{17}$$

It is clear that the use of Eq. (16) largely reduces the possibility of the function $\beta(x)$, and theactive earth pressure is now simply dependent on the factor λ. For a given failure surface, this coefficient could be increased gradually within its possible range to yield the minimum earth pressure and its point of application. Note only those physically reasonable results, which satisfy the condition $0 < (Y_b - T_b) < H$, or an even narrower one based on physical considerations, can be accepted.

It is also feasible to assume an acceptable range for the point of application of the active earth pressure and seek the value of λ that is consistent with the given Tb by solving Eq. (13). Then the obtained λ can be used further in Eq. (11) to calculate the corresponding Gb. This approach was used by Chen and Li (1998) and Chen (2003), however, without finding the local minimum earth pressure for a given failure surface. For this alternative strategy, Eqs. (11) and (15) can be substituted into Eq. (13) to yield the following nonlinear equation without the presence of Gb:

$$\begin{aligned} M_u = &\left[G_a - \int_a^b p(x)s(x)\,\mathrm{d}x\right]t_b + \int_a^b p(x)s(x)t(x)\,\mathrm{d}x \\ &-(T_b - Y_b)\cdot\exp\left[\int_a^b \tan(\varphi - \alpha + \beta)\,\mathrm{d}\beta\right]\cdot\left[G_a - \int_a^b p(x)s(x)\,\mathrm{d}x\right]\cos\beta_b \\ &+(T_a - Y_a)\cdot G_a\cos\beta_a - \int_a^b \frac{\mathrm{d}Q}{\mathrm{d}x}h_e - q\tan\delta(y-z)\mathrm{d}x = 0 \end{aligned} \tag{18}$$

in which Mu denotes the unbalanced moment. It will be shown later that the use of a nonlinear failure criterion for the retained soil may result in a non-monotonic function of Mu(λ) for a given Tb, which may makes the second approach not effective.

2.3. USE OF A NONLINEAR FAILURE CRITERION

For materials with a nonlinear failure criterion, the friction angle mobilized along the failure surface should also be determined during the solution. An extra iteration should be added for this purpose. Once the force angle function β(x) is determined, the inter-slice forces, G(x), can be integrated slice by slice using Eq. (9), and the normal effective stress on each soil slice can be calculated as follows:

$$\sigma_n = \frac{dN}{dx \cdot \sec\alpha} \tag{19}$$

in which the effective normal force, d*N*, can be obtained by using the vertical force equilibrium equation and the failure criterion as given in Eqs. (2) and (3), that is

$$dN = \frac{G_L \sin\beta_L - G_R \sin\beta_R + dW + qdx + u \cdot dx \tan\alpha \tan\varphi - c \cdot dx \tan\alpha}{\left(\cos\alpha + \tan\varphi \sin\alpha\right)} \tag{20}$$

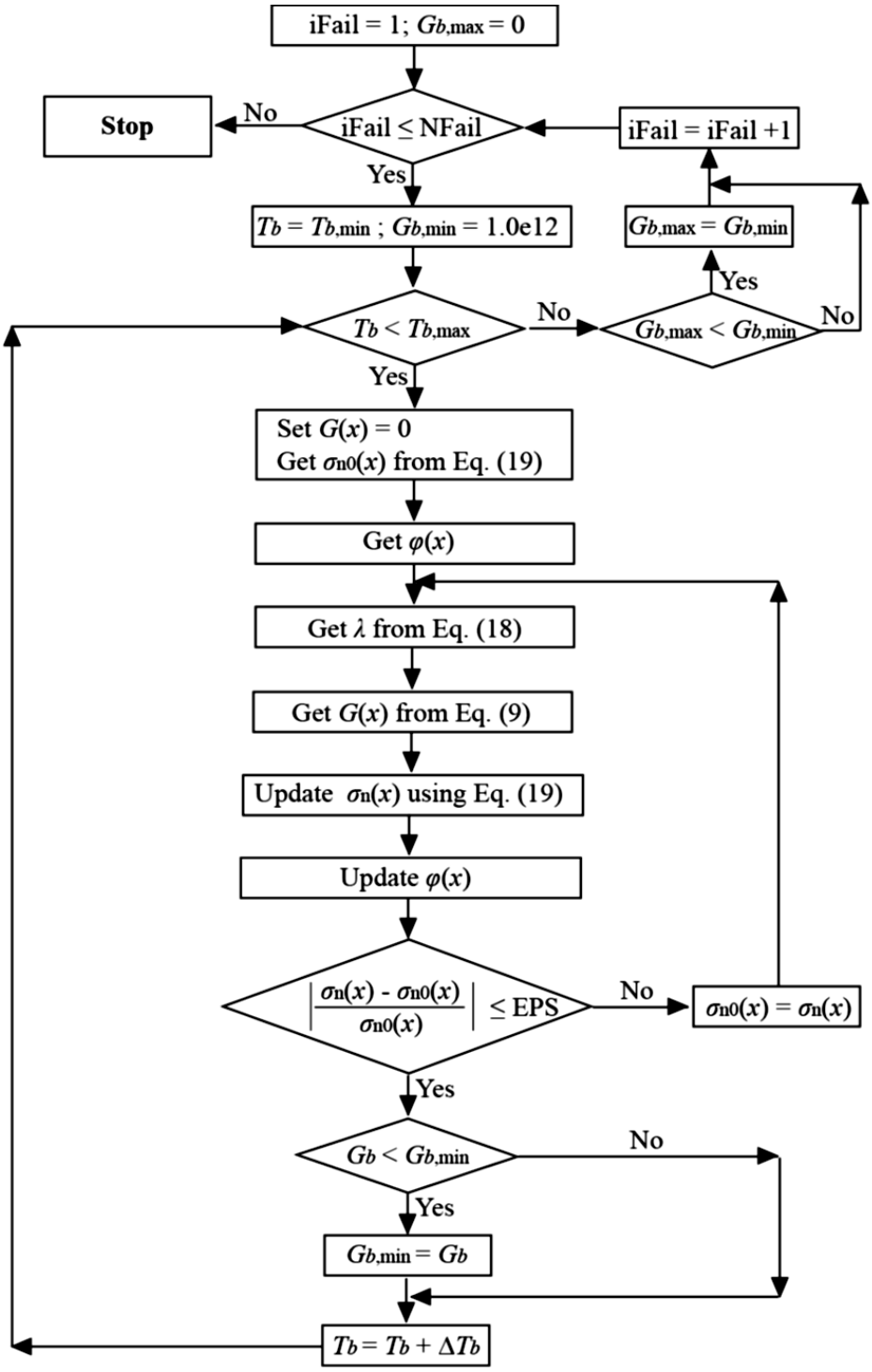

NFail: number of failure surfaces considered; $Tb,\min$ & $Tb,\max$: lower and upper bounds of Tb;
iFail: the counter of failure surfaces; ΔTb: increment of Tb adopted;
$Gb,\max$: global maximum active earth pressure; σ_n & σ_{n0}: normal effective stress;
$Gb,\min$: local minimum active earth pressure; EPS: convergency criteria for iteration.

Fig. 3. Flowchart for seeking the active earth pressure on retaining structures

in which the variables with subscripts L and R denote the interslice forces and their angles applied at the left and right sides of the concerned soil slice. Fig. 3 describes the flowchart of the numerical algorithm for the solution of the active earth pressure. A possible range was prescribed for the point of application (Tb) of the active earth

pressure herein. However, it is sometimes better to set an upper bound and a lower bound for λ and let it the iterative variable instead of T_b. In the latter case, there is no need to solve the nonlinear equation, i.e. Eq. (18). However, the resultant point of application should be verified.

3. VERIFICATION

The algorithm described above was incorporated into a limit equilibrium analysis program LEAPERS (Limit Equilibrium Analysis Program for Earth and Rockfill Structures) developed initially for slope stability problems in earth and rockfill dams (Fu & Chen 2013) based on the generalized method of slices by Chen and Morgenstern (1985) and Chen (2003). Both λ and T_b could be used as the iterative variable during the local minimization process. In this part, same examples were studied to verify and demonstrate the capability of the method and the program.

3.1. SOIL WITH A LINEAR STRENGTH BEHAVIOR

The active earth pressure exerted by a cohesionless soil upon a concrete wall (H =20 m) with a sloping surface was consider first. The unit weight of the soil and its strength parameters as well as the friction angle between the soil and the retaining wall were given in Fig. 4(a). The simplest way to use the vertical soil slices based method for such a sloping retaining structure is to rotate the coordinates so as to keep the retaining surface vertical as shown in Fig. 4(b). Meanwhile, the gravity (g) of each soil slice should be decomposed into a horizontal component, g_x, and a vertical component, g_y, in the rotated system, that is

$$g_x = g\sin\varepsilon;\quad g_y = g\cos\varepsilon \tag{21}$$

in which ε is the angle between the retaining surface and the vertical axis in the original system.

By doing this, the vertical and horizontal components of the gravity can be considered in dW and dQ related terms in Eq. (5), respectively. It should be noted that the boundary conditions for $\beta(x)$ should also be modified accordingly.

The active earth pressure was determined using LEAPERS with plane failure surfaces, and the resultant pressure coefficient ($K_a = G_b/(\gamma H^2/2)$) was plotted against the inclination angle of the failure surface, α, and the coefficient λ in Fig. 5(a). The variations of K_a and the corresponding point of application ($(Y_b\text{-}T_b)/H$) with λ for the critical (most dangerous) failure surface were also plotted in Fig. 5(b). Both the critical failure surface and the corresponding active earth pressure obtained herein coincide exactly with Coulomb's theoretical solutions. In addition, it is interesting to note that K_a was not influenced by λ for a given α in this particular case. This feature can be explained by simplifying Eq. (10) with a constant φ and α, that is

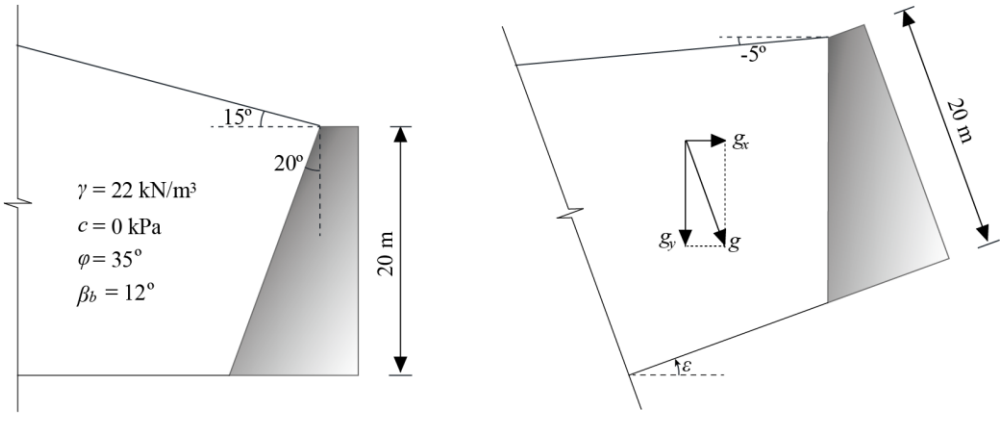

(a) in the original coordinate system (b) in the rotated coordinate system

Fig. 4. The active earth pressure problem on a sloping retaining surface

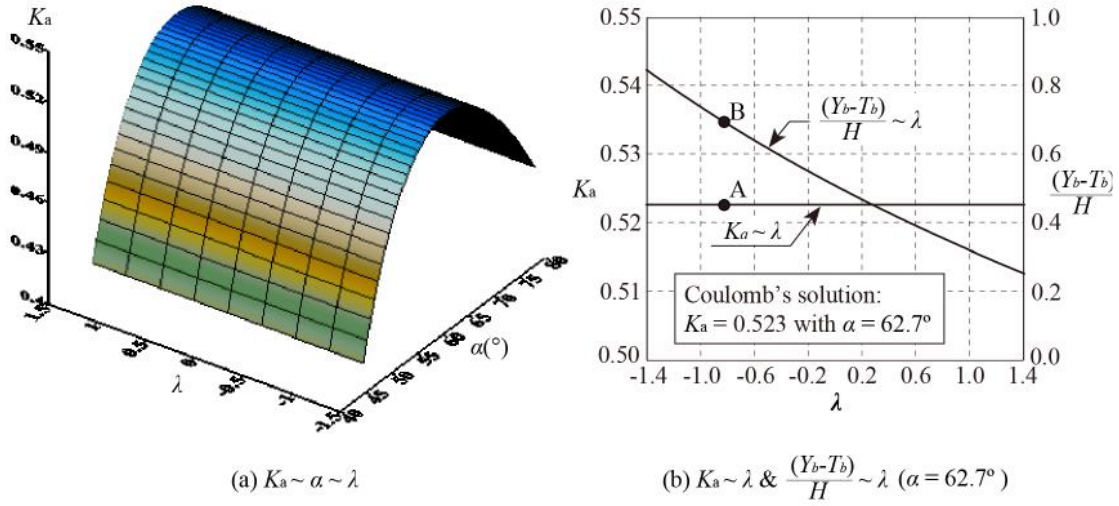

(a) $K_a \sim \alpha \sim \lambda$ (b) $K_a \sim \lambda$ & $\frac{(Y_b-T_b)}{H} \sim \lambda$ ($\alpha = 62.7°$)

Fig. 5. The variation of the active earth pressure and its application point with α and λ (based on linear strength parameters: c = 0 and φ = 35°)

$$s(x) = \sec(\varphi - \alpha + \beta_a) \tag{22}$$

Therefore, Eq. (11) can be reduced to the following form:

$$G_b = \frac{\cos(\varphi - \alpha + \beta_a)}{\cos(\varphi - \alpha + \beta_b)} \cdot \left[G_a - \sec(\varphi - \alpha + \beta_a) \int_a^b p(x)\,dx \right] \tag{23}$$

which is a function depends only on the loads and the friction angle between the wall and the soil (βb), but not influenced by the $\beta(x)$ distribution within the soil mass. This conclusion, however, is valid only for a plane failure surface in a single soil stratum. Even in such a simple condition, the strength mobilized along the vertical sides of the soil slices does affect the application point of the earth presure. For instance, if the wall cannot sustain the pressure indicated by A that applied at a point indicated by B as shown in Fig. 5(b), then it will deform away from the retained soil, which in turn results in a downward movement of the point of application, but preserving the amount of active earth pressure.

Since the change of the point of application does not alter the amount of active earth pressure for a given plane failure surface, the point of application cannot be determined in this method. This conclusion is exactly like the fact that Coulomb's earth pressure theory in itself cannot predict the point of application of the active earth pressure (Fu et al. 2014; Sun and Song 2016).

3.2. SOIL WITH A NONLINEAR STRENGTH BEHAVIOR

The previous problem shown in Fig. 4 was used as the first example in this subsection. Eq. (1) was employed for the retained soil so as to reflect the nonlinear strength behavior. However, the confining pressure $\sigma 3$ in Eq. (1) was replaced tentatively by the normal effective stress, σn, along the failure surface. Use of the nonlinear strength parameters was discussed later. Herein, the two parameters for the peak friction angle were $\varphi 0$ = 45° and $\Delta\varphi$ = 8°. Other parameters were the same as those in Fig. 4. In order to compare with the results in Fig. 5, only plane failure surfaces were considered in this case.

Fig. 6(a) shows the variation of K_a with α and λ, and Fig. 6(b) plots the particular results for the critical failure surface (α = 69.3°). Differently from the results shown in Fig. 5, K_a is evidently influenced by the value of λ and hence the point of application for any given failure surface. In addition, for each failure surface there is a clear local minimum of K_a that could be attained when λ approaches a certain value as illustrated in Fig. 5(b), either an increase or a decrease of λ from this stationary point will result in an increase of the active earth pressure.

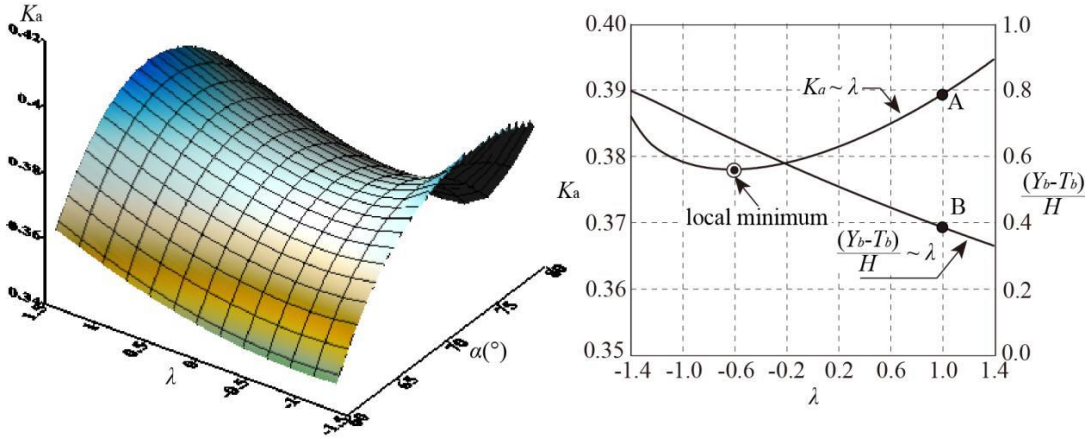

(a) $K_a \sim \alpha \sim \lambda$ (b) $K_a \sim \lambda$ & $\frac{(Y_b-T_b)}{H} \sim \lambda$ $(\alpha = 69.3°)$

Fig. 6. The variation of the active earth pressure and its application point with α and λ (based on nonlinear strength parameters: $\varphi_0 = 45°$ and $\Delta\varphi = 8°$)

Variation of the active earth pressure and its point of application with the interslice force angles reflects the fact that the soil-retaining wall system has a flexibility to adjust the internal forces so as to sustain an overall stability. For instance, if the interslice forces initially follow a distribution corresponding to $\lambda = 1.0$, then, to keep the soil mass stable, the retaining wall should provide a force, the amount and application point of which were denoted by A and B in Fig. 5(b). However, the retaining wall itself may not be able to keep stable under such a high earth pressure, and it tends to displace or deform away from the retained soil. Such a tendency will result in a change of the earth pressure and an adjustment of the application point. The soil, on the hand, should also adjust the internal forces to keep itself stable. Such a mutual adjustment of earth pressure and soil strength mobilization will cease if and only if the retaining wall can sustain the minimal earth pressure without losing stability. This is the reason why for a given failure surface the minimal earth pressure is meaningful but not the maximum. However, for all the possible failure surfaces, the retaining wall can keep stable if and only if it can sustain the maximum of those minimal earth pressures. Therefore, the active earth pressure problem is mathematically finding the so-called saddle point on a surface demonstrated in Fig. 6 (a).

The second example demonstrated in this subsection is the active earth pressure problem studied by both Yang (2007) and Sun and Song (2016) based on the limit analysis method and the slip line method, respectively. The retaining wall was assumed smooth and vertical, and the following nonlinear failure criterion was used for the retained soil:

$$\tau = c_0 \left(1 + \frac{\sigma_n}{\sigma_t}\right)^{\frac{1}{m}} \qquad (24)$$

in which σ_n and τ are the normal and the shear stresses on the failure surface, c_0, σ_n and m are three parameters. The surface of the soil was horizontal and no surcharge was applied.

Table 1 and Table 2 compares the results obtained using different methods. Note that an additional horizontal acceleration ($a_h = 0.98 m/s^2$) was considered in the cases listed in Table 2. In most of the cases, the results obtained by the present method agree well with those by Sun and Song (2016), and are slight higher than the ones by Yang (2007). These minor deviations may be caused by different shapes used for the failure surfaces. Herein, circular failure surfaces were used, while quadratic and log-spiral surfaces were assumed in Sun and Song (2016) and Yang (2007), respectively.

Table 1 Comparison of static active earth pressures acting on a smooth and vertical wall

Active earth pressure (kN/m)	Coefficient m				
	1.2	1.4	1.6	1.8	2.0
Present method	25.56	32.19	37.56	41.79	45.30
Sun and Song (2016)	23.30	31.16	37.29	41.28	43.88
Yang (2007)	22.53	28.87	34.01	38.41	41.98

H = 4.0m, c_0 = 9 kPa, σ_t = 20 kPa, γ = 18 kN/m^3.

Table 2 Comparison of dynamic active earth pressures acting on a smooth and vertical wall

Active earth pressure (kN/m)	Coefficient m				
	1.2	1.4	1.6	1.8	2.0
Present method	36.19	43.83	49.86	54.63	58.46
Sun and Song (2016)	34.35	42.04	49.32	55.13	59.96
Yang (2007)	32.66	39.78	45.61	50.39	54.32

H = 4.0m, c_0 = 9 kPa, σ_t = 20 kPa, γ = 18 kN/m^3, a_h = 0.98m/s^2.

The satisfactory solutions obtained for the above examples prove that the slices-based limit equilibrium method is reliable in evaluating the static and dynamic active earth pressure exerted upon vertical or sloping retaining walls by soils with either linear or nonlinear failure strength behavior. In the following part, some topics related to the slices-based limit equilibrium method were discussed further.

4. DISCUSSIONS ON THE SLICES-BASED METHOD

All the examples demonstrated previously were studied using the assumption in Eqs. (16) and (17). In this part, another two continuous $f(x)$ functions were used for the construction of $\beta(x)$, i.e.

$$f(x)=\begin{cases}\sin\dfrac{2\pi}{b-a}(x-a) & \dfrac{x-a}{b-a}\le\dfrac{1}{4}\\ \sin\left[\dfrac{\pi}{3}+\dfrac{2\pi}{3(b-a)}(x-a)\right] & \dfrac{x-a}{b-a}>\dfrac{1}{4}\end{cases} \tag{25}$$

and

$$f(x)=\begin{cases}\sin\dfrac{2\pi}{3(b-a)}(x-a) & \dfrac{x-a}{b-a}\le\dfrac{3}{4}\\ \sin\left[\dfrac{2\pi}{(b-a)}(x-a)-\pi\right] & \dfrac{x-a}{b-a}>\dfrac{3}{4}\end{cases} \tag{26}$$

Both functions were shown in Fig. 7 together with the one given in Eq. (17). Eq. (25) shifts the peak to the coordinate $x = a + (b\text{-}a)/4$, while Eq. (26) moves it to $x = a + 3(b\text{-}a)/4$.

4.1. PREFERENCE OF THE ITERATIVE VARIABLE FOR LOCAL MINIMIZATION PROCESSES

As was pointed out previously, both the coefficient λ and the point of application T_b could be used as the iterative variable for the local minimization processes. Herein, it will be shown that for soils with linear strength behavior the minimization process is not necessary essentially. However, some subtle difference may exist when a nonlinear failure criterion was used for the retained soil, and there would be a preference for different problems.

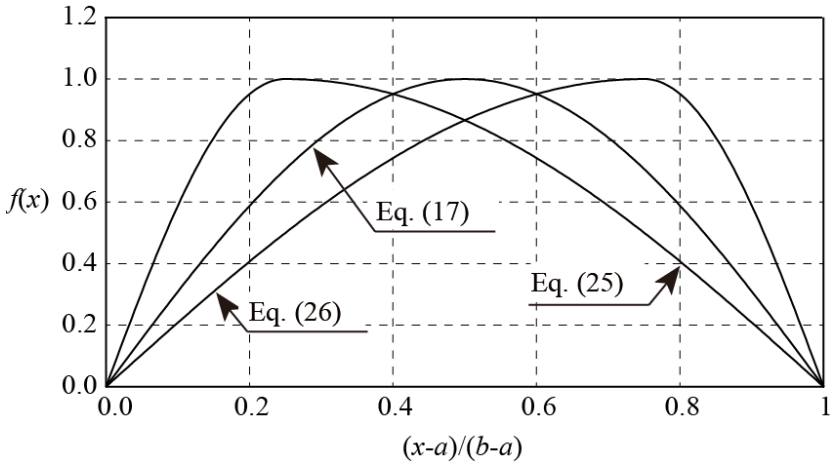

Fig. 7. The f(x) functions given by Eqs. (17), (25) and (26)

The example shown in Fig. 4 was studied again here to clarify the above argument. First, the linear failure criterion was used ($\varphi = 35°$). Fig. 8(a) shows the variation of the unbalanced moment Mu with the coefficient λ for a particular failure surface (the critical circular one based on Eq. (17) and a given point of application, i.e., (Yb-Tb)/H = 0.5. No matter which function was used for f(x), the unbalanced moment increases monotonically with λ, and there is only one particular λ that makes the unbalanced moment vanishing (Mu = 0). This characteristic is quite beneficial for solving Eq. (18). Fig. 8(b) ~ (d) plots the mutual relationships between the coefficient λ, the active earth pressure coefficient and the point of application for this critical failure surface. A continuous increase of λ results in a monotonic decrease of the active earth pressure and meanwhile a continuous descending of the point of application as shown in Fig. 8(b) and Fig. 8(c).

Furthermore, it is interesting to note that for a given point of application, the resultant active earth pressures predicted with three f(x) functions are almost the same as shown in Fig. 8(d). This finding can be explained by the fact that the critical circular failure surface is steep and very close to a plane one and therefore the active earth pressure is almost not influenced by $\beta(x)$ as verified in Section 3.1.

It also deserves to point out that no stationary points exist on the curves plotted in Fig. 8(b) and Fig. 8(d), and the local minimum active earth pressure can only be attained at the specified upper bound of λ or the lower bound of (Yb-Tb)/H. The local minimization process, therefore, is in fact not necessary for soils with linear strength behavior. Instead, the upper bound of λ or the lower bound of (Yb-Tb)/H could be specified directly. Since the point of application has a clearer physical meaning and the bound of which can be judged more easily according to the flexibility of the retaining structures (Chen 2003), we suggest using the lower bound of the latter for the evaluation of the active earth pressure. The fact that given a point of application the active earth pressure is almost independent of the selection of f(x) (Fig. 8(d)) serves as an additional reason for this suggestion.

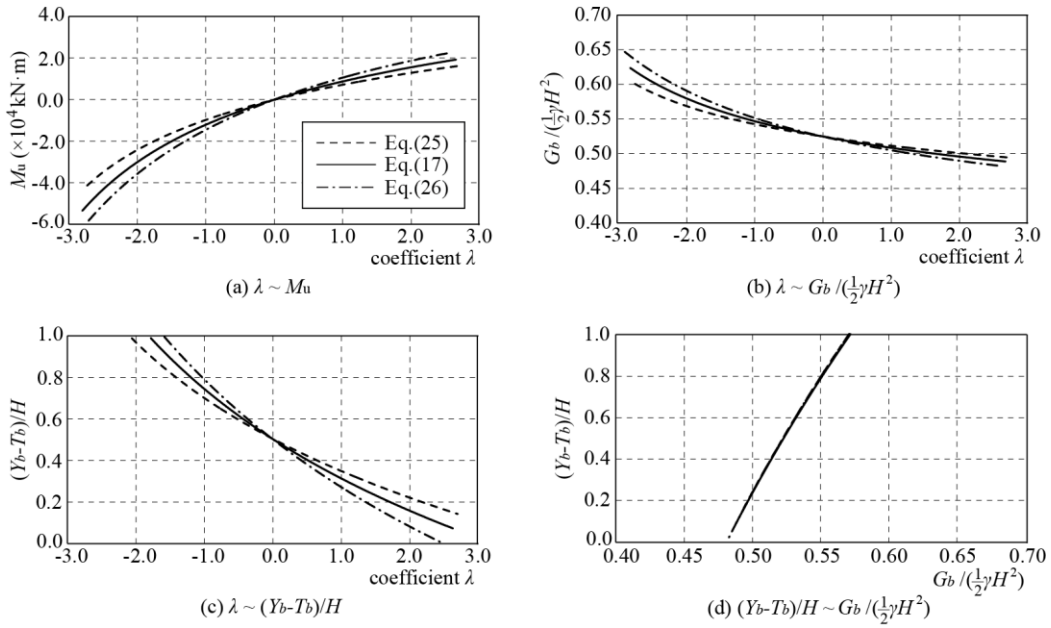

Fig. 8. The influences of λ on the unbalanced moment and the active earth pressure as well as its point of application for a given circular failure surface (c = 0, φ = 35°)

To study the counterparts of the curves plotted in Fig. 8 for soils obeying a nonlinear failure criterion. Eq. (1) was used again with σ3 replaced by σn. φ0 and Δφ were set to 54.0° and 11.6°, respectively, which were among the typical ranges of rockfill materials. The failure surface used was the critical one corresponding to (Yb-Tb)/H = 0.66 without local minimization processes. Fig. 9(a) plots the unbalanced moment Mu against the coefficient λ. Only the Mu predicted with Eq. (25) increases monotonically with λ while the Mu predicted with Eq. (17) and Eq. (26) experienced an initial decrease and a subsequent increase when λ was increased continuously. In particular, the Mu~λ curve predicted with Eq. (17) has two points satisfying Mu = 0 while the one by Eq. (26) has no solution for this nonlinear equation. These characteristics can result in numerical difficulty in obtaining converged or reliable solutions for some given Tb. Although such numerical difficulty may not always present for all failure surfaces, it cannot be judged in advance.

The curves plotted in Fig. 9(b) demonstrate again the existence of local minimum active earth pressures and therefore the necessity of performing local minimization processes, when the retained soil exhibits a nonlinear strength behavior. As the solution of Eq. (18) may not be unique for a given Tb, it is possible to obtain an unreliable active earth pressure if no local minimization was employed. Take the curves corresponding to Eq. (26) as an example, there are two possible values of λ that satisfy the condition (Yb-Tb)/H = 0.6 for the current failure surface, as indicated by A and B in Fig. 9(c). It is very possible that the solution denoted by B be obtained due to the selection of the initial guess of λ, and hence the high active earth pressure denoted by B in Fig. 9(d) be recorded. Because the global maximization process is to seek the maximal value of Gb, it is very likely that the active earth pressure indicated by point B be finally picked, which, of course, overestimates the real active earth pressure. Selecting other f(x) functions makes no guarantee to avoid such a possible dilemma. Therefore, for soils with nonlinear strength behavior, we suggest using the coefficient λ as the iterative variable and always performing a local minimization process for each possible failure surface, so that the unreasonable solutions such as the one denoted by point B can be discarded.

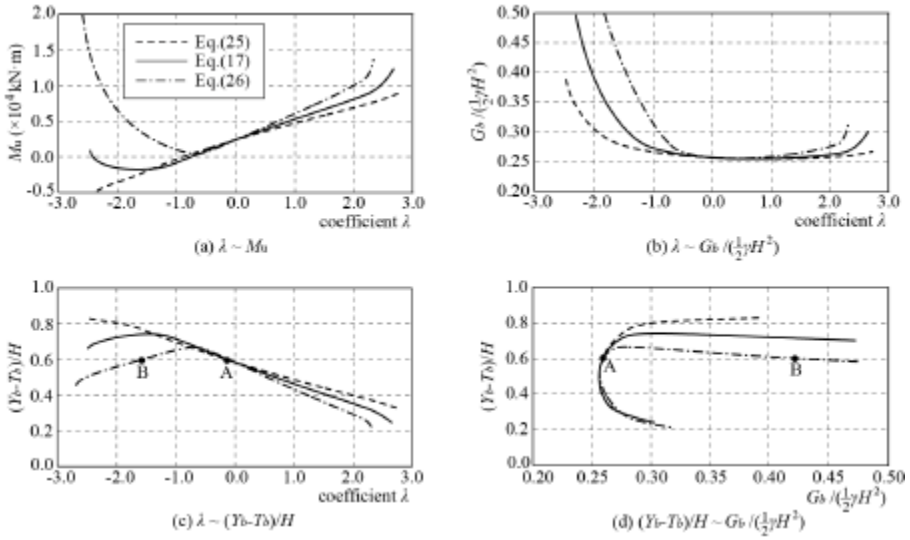

Fig. 9. The influences of λ on the unbalanced moment and the active earth pressure as well as its point of application for a given circular failure surface (φ0 = 54°, Δφ = 11.6°)

The possible range of λ can be obtained by specifying the maximum interslice force angle according to the shear strength of the retained soils. It is also necessary to provide an allowable range for the point of application of the active earth pressure based on the flexibility of the retaining structures. 4.2 Influence of β(x) on the active earth pressure.

4.2. INFLUENCE OF B(X) ON THE ACTIVE EARTH PRESSURE

To clarify the influence of the interslice force angle function β(x) on the active earth pressure further, Eqs. (17), (25) and (26) were used in conjunction with Eq. (16) to study the problem stated in Fig. 6 again. Both plane failure surfaces and circular failure surfaces were used herein. Fig. 10 shows the locations of the critical failure surfaces (y=y(x)) and the lines of thrust (y=yt(x), lines formed by connecting the points of application of G(x)) as well as the values of the active earth pressure predicted.

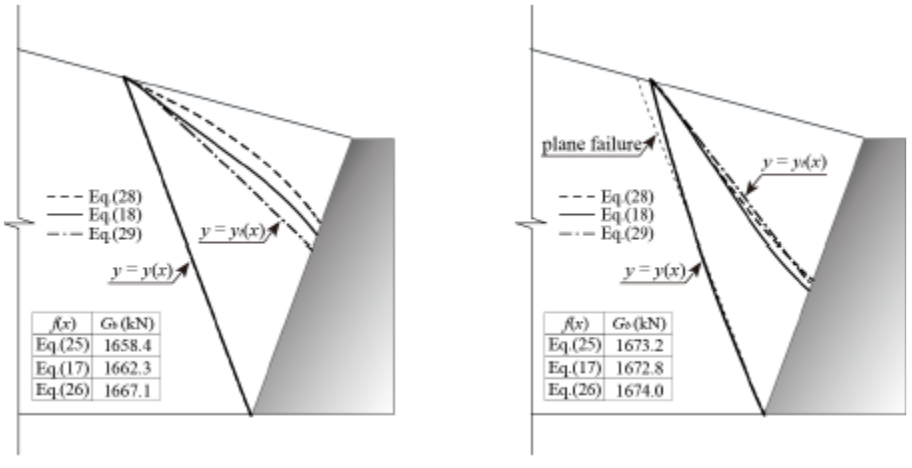

Fig. 10. The failure surfaces (y=y(x)), lines of thrust (y=yt(x)) and the active earth pressures predicted using Eqs. (17), (25) and (26)

The locations of the critical failure surfaces, either the plane ones or those circular ones, are almost the same regardless of the f(x) functions used in Eq. (16). For both types of surfaces, the differences between the active earth pressures predicted with different f(x) functions are negligible, with the maximum deviations not exceeding 1%. This is an evidence that the active earth pressure is almost not influenced by the interslice force angles. Furthermore, the circular critical failure surface as well as the magnitude of the active earth pressure are also very close to those of the plane one as shown in Fig. 10. That is to say a plane failure surface is acceptable in

evaluating the active earth pressure exerted by soils with a nonlinear failure criterion, at least for a first approximation. However, it should be noted that the lines of thrust and the point of application of the active earth pressure are clearly influenced by the selection of f(x) functions and the type of failure surfaces. A circular failure surface generally results in a lower line of thrust and also a lower point of application compared with those for plane failure surfaces. In addition, the influence of the f(x) function on the lines of thrust is more evident for plane failure surfaces than that for circular ones.

The detailed distributions of G(x), σn(x), β(x) and φ(x) corresponding to the results shown in Fig. 10 were plotted in Fig. 11 and Fig. 12, respectively. The abscissa in these figures is the relative distance of the concerned point measured from the left boundary (x=a) towards the retaining surface (x=b). For both types of failure surfaces, the interslice force, G(x), increases monotonically from the left boundary to the retaining surface, with the influence of function f(x) more evident near the center of the sliding mass than that near the both boundaries, as shown in Fig. 11(a) and Fig. 12(a). Despite of the small difference between the active earth pressures predicted for plane and circular failure surfaces, the distributions of normal stress, σn(x), exhibit more considerable deviations. In Fig. 11(b) the normal stress σn increases initially with the relative distance until a peak is attained. After that point the normal stress σn decreases gradually until the retaining surface is reached. This particular distribution results in an initial decrease and a subsequent increase of the mobilized friction angle along the failure surface as shown in Fig. 11(d). Differently, the normal stress σn along the circular failure surface increases monotonically from the left boundary to the retaining wall, yielding a continuous decrease of the mobilize friction angle along the failure surface as shown in Fig. 12 (b) and (d).

Although the values of the active earth pressure predicted with different f(x) functions are very close to each other for a given failure surface, the interslice force angles along the sides of soil slices, β(x), may show considerable difference, as demonstrated in Fig. 11(c) and Fig. 12(c). As a result, the normal stress and the mobilized friction angle along the failure surface also differ from each other as shown in Fig. 11 and Fig. 12. It is the versatility of the backfilled soil in adjusting the interslice forces and the stresses along the failure surface according to the interslice force angle distributions that makes the minimum force required to keep the sliding mass stable almost not changed by β(x). Examples studied herein also demonstrate the applicability of Eqs. (16) and (17) in earth pressure problems, even if the retained soil obeys a nonlinear failure criterion.

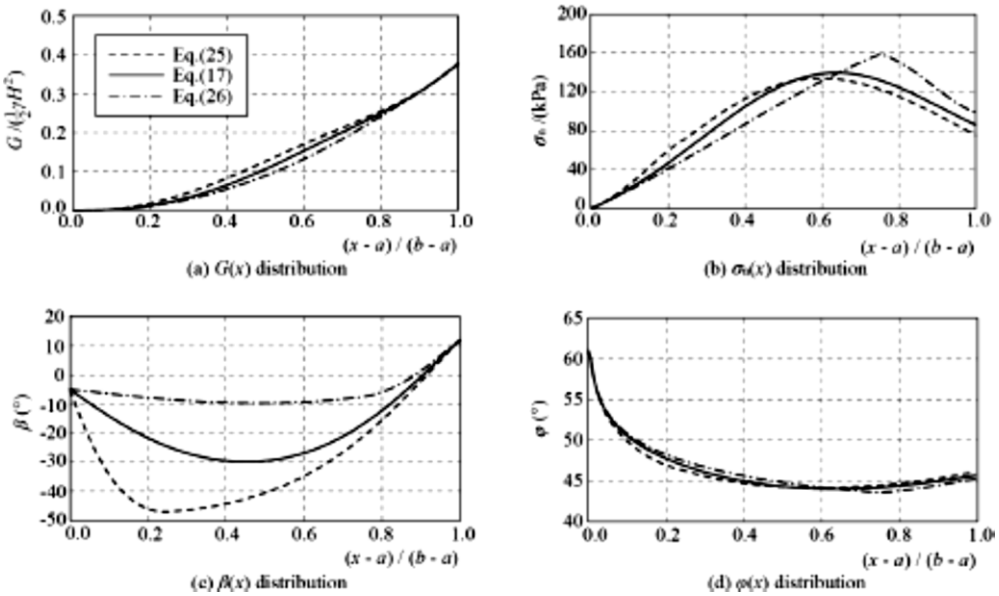

Fig. 11. The distributions of G(x), σn(x), β(x) and φ(x) (using a plane failure surface)

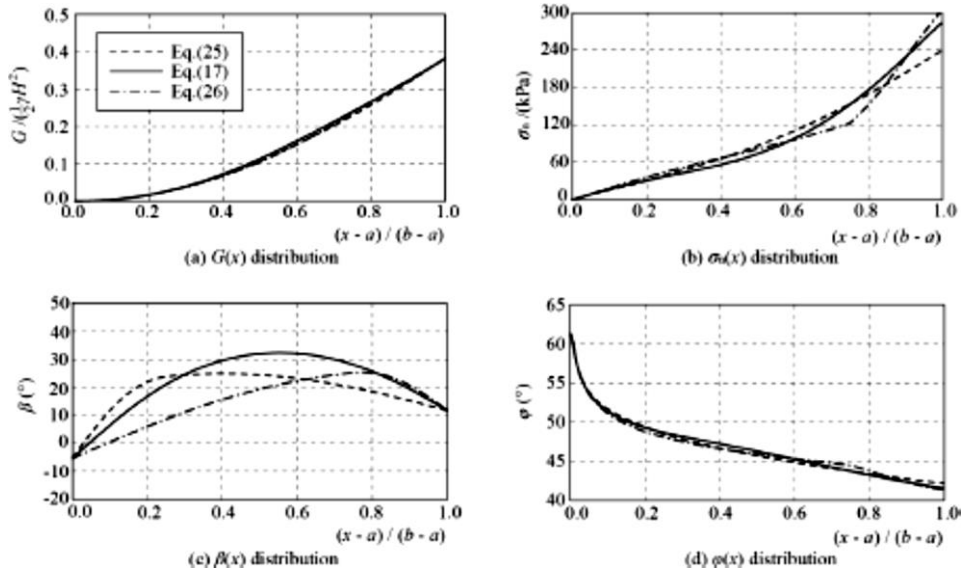

Fig. 12. The distributions of G(x), σn(x), β(x) and φ(x) (using a circular failure surface)

4.3. DETERMINATION OF NONLINEAR STRENGTH PARAMETERS

In geotechnical practice, two types of experiments are most widely used in determining the strength of soils, i.e. direct shear experiments and triaxial compression experiments (Smith and Smith 1998). Definitions of the friction angle in both experiments are not the same. In direct shear experiments, the friction angle is defined as $\varphi = \tan^{-1}(\tau n/\sigma n)$, and it is evaluated in triaxial experiments by $\varphi = \sin^{-1}[(\sigma 1-\sigma 3)/(\sigma 1+\sigma 3)]$. Note cohesionless soils are considered here. It can be seen from Eq. (3) that in the slices-based limit equilibrium method, the definition used in direct shear experiments is inherently used. However, for soils with linear strength behavior, the friction angles obtained by triaxial compression experiments can be used equivalently because $\tan^{-1}(\tau n/\sigma n) = \sin^{-1}[(\sigma 1-\sigma 3)/(\sigma 1+\sigma 3)]$.

For soils with nonlinear strength behavior, cautions should be exercised on the experiments and the way to establish the failure envelope. Take the one given in Eq. (24) as an example, if it was based on direct shear experiments, then the relevant parameters can be used directly. However, if triaxial experiments were conducted to determine the parameters, attentions should be paid. It is a common practice in geotechnical engineering that the common tangent of a series of Mohr circles be defined as the strength envelope as illustrated by the solid curve in Fig. 12. The points sampled in this way do not coincide with those where the shear stress ratio ($\tau n/\sigma n$) achieves a maximum. For instance, point A on the largest Mohr circle is sampled to construct the strength envelope, however, the shear stress ratio achieves a maximum at point B, which is not the same as point A. To be consistent with the strength definition in slices-based limit equilibrium method, point B should be sampled from this particular Mohr circle, instead of point A. The final strength envelope thus obtained will be slightly lower than the common tangent as shown in Fig. 12 (the dashed curve). For soils with a linear strength envelope, the points on the common tangent always coincide with those points where the shear stress ratio achieves a maximum, therefore the parameters can be used directly.

Based on the above considerations, the easiest way to obtain a nonlinear strength envelope and the relevant parameters for active earth pressure problems using the current method is to conduct direct shear experiments (Matsuoka and Liu 1998; Oyangurena et al. 2008; Liu 2009;) and plot the peak friction angle or the peak shear stress against the vertical normal stress. On the other hand, if triaxial compression experiments were performed and a series of Mohr circles were at hand, it is also simple to convert them to the normal stress ~ maximum shear stress pairs. To this end, the equation for the Mohr circle is used, i.e.

$$\tau = \sqrt{(\sigma_1 - \sigma)(\sigma - \sigma_3)} \tag{27}$$

Therefore, the shear stress ratio could be expressed as follows:

$$\frac{\tau}{\sigma} = \sqrt{\left(\frac{\sigma_1}{\sigma} - 1\right)\left(1 - \frac{\sigma_3}{\sigma}\right)} \tag{28}$$

At the maximum shear stress ratio point, the following stationary condition should be fulfilled:

$$\frac{\mathrm{d}(\tau/\sigma)}{\mathrm{d}\sigma} = 0 \tag{29}$$

from which the normal stress can be obtained, i.e.

$$\sigma_n = \frac{2\sigma_1\sigma_3}{\sigma_1 + \sigma_3} \tag{30}$$

Substituting the normal stress obtained into Eq. (27) yields the corresponding shear stress τ_n, and then a failure envelope can be constructed based on these (σ_n, τ_n) pairs.

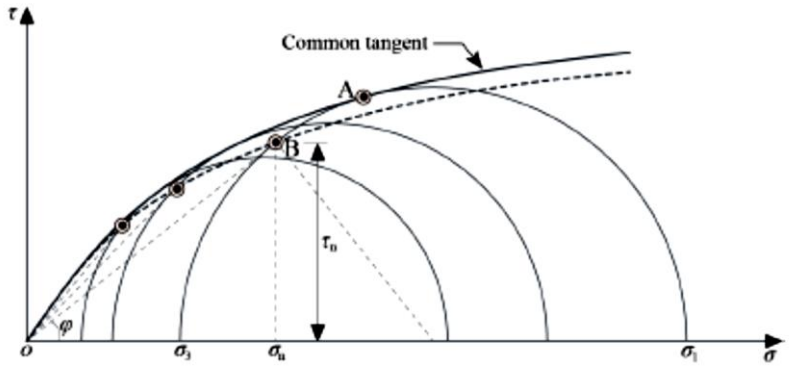

Fig. 12. The strength envelope based on triaxial experiments

5. CONCLUSIONS

In this paper, we demonstrated the applicability of the slices-based limit equilibrium method in evaluating the active earth pressure applied by soils with nonlinear strength behavior. Two extensions to the original method for soils with linear strength behavior were made. First, an iterative process was performed for the normal effective stress along the failure surface, so that the peak friction angle mobilized is consistent with the normal effect stress. Second, a local minimization process was employed for each possible failure surface, so that the unreasonable results can be discarded. The following conclusions can be summarized based on the current research:

(1) The active earth pressure is a functional depends on the location of the failure surface and the distribution of interslice force angles. Mathematically, solving an active earth pressure problem is seeking the saddle point of a surface. At this particular point, a maximum active earth pressure of a series of minimum ones is achieved. The local minimums can be obtained by varying the distribution of interslice force angles, and the global maximum is the one corresponding to the critical failure surface.

(2) Introducing an assumption (Eq. (16)) for the interslice force angle distribution largely simplifies the processes of seeking a maximum from minimums. The variational problem in the function space is simplified into an extreme problem in the real space. In addition, for soils with linear strength behavior, the active earth pressure for a given failure surface decreases continuously as the point of application is lowered. Therefore, the local minimums can only be achieved at the lower boundary of the application point and the minimization process is actually not needed. However, for soils with nonlinear strength behavior, local minimums do exist and the nonlinear equation for moment equilibrium may become non-monotonic and ill-shaped, which adds difficulty in obtaining a converged and reliable solution. Therefore, the coefficient λ in Eq. (16) is suggested to be used for the local minimization processes.

(3) The distribution of interslice force angle, $\beta(x)$, influences the normal stress distribution and the mobilized friction angle along the failure surface. However, the resultant active earth pressure applied on the retaining surface is almost not influenced. In particular, for soils obeying a linear failure criterion, the active earth

pressures predicted with different f(x) functions are almost the same for a given point of application. For soils with nonlinear strength behavior, however, the lines of thrust and the application points of the active earth pressure are clearly influenced by f(x) and β(x), particularly when plane failure surfaces were used. The lines of thrust and the points of application predicted for circular failure surfaces are generally lower than those for plane failure surfaces. However, the critical failure surface and the corresponding active earth pressure are very close to each other, indicating the feasibility of using plane failure surfaces for the evaluation of the active earth pressure by soils with nonlinear strength behavior.

(4) In the slices based limit equilibrium method, the peak friction angle is defined using the normal and shear stresses along the maximum shear stress ratio plane, which is consistent with the direct shear experiments. When the nonlinear strength envelope is constructed using triaxial compression experiments, cautions should be exercised. If the common tangent of a series of Mohr circles is draw to represent the strength envelope, then the parameters cannot be used directly. Conversion of the experimental data ((σ1, σ3) pairs) to the normal and shear stresses pairs (σn, τn) is required.

It deserves to point out finally that the assumption used for the interslice force angles evidently reduced the possibility of the distribution of interslice force angles. Exclusion of other possible distributions means the local minimum active earth pressure obtained may not be the real minimum one. That is to say the local minimum active earth pressure obtained with a given distribution of the interslice force angles is always a conservative one, the maximum of which may lead to a conservative design in engineering practice.

6. ACKNOWLEDGEMENT

This work was supported by the national Natural Science Foundation of China (NSFC, Grant Nos. 51539006 & 51379130). The financial support from the Ministry of Water Resource (MWR, Grant No. 201501035) was also greatly appreciated.

7. REFERENCES

1. Andrews L C, Phillips R L. Mathematical Techniques for Engineers and Scientists. SPIE Press, Washington, 2004.
2. Benmeddour D, Mellas M, Frank R, Mabrouki A. Numerical study of passive and active earth pressures of sands. Computers and Geotechnics, 2012, 40: 34-44.
3. Bhatia S K, Bakeer R M. Use of the finite element method in modelling a static earth pressure problem. International Journal for Numerical and Analytical Methods in Geomechanics, 1989, 13(2): 207-213.
4. Chen W F. Limit Analysis and Soil Plasticity. Elsevier, Amsterdam, 1975.
5. Chen Z Y, Li S M. Evaluation of active earth pressure by the generalized method of slices. Canadian Geotechnical Journal, 1998, 35(4): 591-599.
6. Chen Z Y, Morgenstern N R. Extensions to the generalized method of slices for stability analysis. Canadian Geotechnical Journal, 1983, 20(1): 104-119.
7. Chen Z Y. Soil Slope Stability Analysis, Theory, Methods and Programs. China Water & Power Press. Beijing, 2003.
8. Collins I F, Gunn C I M, Pender M J, Yan W. Slope stability analyses for materials with a non-linear failure envelope. International Journal for Numerical and Analytical Methods in Geomechanics, 1988, 12(5): 535-550.
9. Fu Z Z, Chen S S. Limit Equilibrium Analysis Program for Earth and Rockfill Structures (LEAPERS). Theory and Manual. Report of Nanjing Hydraulic Research Institute. Nanjing,2013
10. Fu Z Z, Li G Y. Three-Dimensional Finite Element Analysis of the Behavior of the Jiayan Concrete Face Rockfill Dam in Yunnan Province, China. Scientific Report of Nanjing Hydraulic Research Institute (No. HJ312029), Nanjing, 2012.
11. Fu Z Z, Wang Z J, Chen S S. Calculation method for earth pressure and stability of high submerged toe walls of concrete faced rockfill dams. Hydro-Science and Engineering, 2014, 3: 1-8.
12. Jiang J C, Baker R, Yamagami T. The effect of strength envelope nonlinearity on slope stability computations. Canadian Geotechnical Journal, 2003, 40(2): 308-325.
13. Kreyszig E. Advanced Engineering Mathematics (Tenth Edition). John Wiley & Sons. Jefferson City, Missouri, 2010.

14. Leps T M. Review of shearing strength of rockfill. Journal of the Soil Mechanics and Foundation Division, 1970, 96(4): 1159-1170.
15. Liu F Q, Wang J H. A generalized slip line solution to the active earth pressure on circular retaining walls. Computers and Geotechnics, 2008, 35(2): 155-164.
16. Liu S H, Fu Z Z, Yang J Z. Back analysis of deformation parameters of rockfills in a pumped storage station project. In: Proceedings of the 1st International Conference on Long Term Effects and Seepage Behavior of Dams (eds. Zhu Y M & Liu S H). pp. 23-30, 2008.
17. Liu S H. Application of in situ direct shear device to shear strength measurement of rockfill materials. Water Science and Engineering, 2009, 2(3): 48-57.
18. Maksimovic M. Nonlinear failure envelope for soils. Journal of Geotechnical Engineering, 1989, 115(4): 581-586.
19. Matsuoka H, Liu S H. Simplified direct box shear test on granular materials and its application to rockfill materials. Soils and Foundations, 1998, 38(4): 275-284.
20. Oyangurena P R, Niciezab C G, Fernándezb M I, Palaciob C G. Stability analysis of Llerin dam: an in situ direct shear test. Engineering Geology, 2008, 100(3-4): 120-130.
21. Peng M X, Chen J. Slip-line solution to active earth pressure on retaining walls. Géotechnique, 2013, 63(12): 1008-1019.
22. Potts D M, Fourie A B. A numerical study of the effects of wall deformation on earth pressures. International Journal for Numerical and Analytical Methods in Geomechanics, 1986, 10(4): 383-405.
23. Rahardjo H, Fredlund D G. General limit equilibrium method for lateral earth force. Canadian Geotechnical Journal, 1984, 21(1): 166-175.
24. Smith G N, Smith I G N. Elements of Soil Mechanics (7^{th} Edition). Blackwell Science, London, 1998.
25. Sun Y J, Song E X. Active earth pressure analysis based on normal stress distribution function along failure surface in soil obeying nonlinear failure criterion. Acta Geotechnica, 2016, 11(2): 255-268.
26. Worden F T, Achmus M. Numerical modeling of three-dimensional active earth pressure acting on rigid walls. Computers and Geotechnics, 2013, 51: 83-90.
27. Xiao Y, Liu H L, Chen Y M, Jiang J S. Strength and deformation of rockfill material based on large-scale triaxial compression tests. I: Influence of density and pressure. Journal of Geotechnical and Geoenvironmental Engineering, 2014, 140(12): 10.1061/(ASCE)GT.1943- 5606.0001176, 04014070.
28. Yang X L. Upper bound limit analysis of active earth pressure with different fracture surface and nonlinear yield criterion. Theoretical and Applied Fracture Mechanics, 2007, 47(1): 46-56.
29. Zakerzadeh N, Fredlund D G, Pufahl D E. Interslice force functions for computing active and passive earth force. Canadian Geotechnical Journal, 1999, 36(6): 1015-1029.
30. Zhang X J, Chen W F. Stability analysis of slopes with general nonlinear failure criterion. International Journal for Numerical and Analytical Methods in Geomechanics, 1987, 11(1): 33-50.